Macromolecules 1987, *20*, 2633–2634

Low-Angle Scattering from Flexible, Free-Draining Polymers in Homogeneous Flows

D. A. HOAGLAND

Department of Polymer Science and Engineering,
University of Massachusetts,
Amherst, Massachusetts 01003. Received April 13, 1987

Low-angle scattering techniques have been widely employed to determine the size, shape, and orientation of macromolecules with nonequilibrium conformations. The change in molecular conformation during deformation of a macroscopic sample, for example, can be monitored with either light or neutron scattering. Many investigators have chosen to characterize the stressed conformations produced in deformation experiments using the "radii of gyration" perpendicular and parallel to the direction of molecular extension. It is the purpose of this note to present calculations of the low-angle scattering intensities for Rouse chains in flow. The calculations will demonstrate the limitations of low-angle scattering for the study of molecular deformation in solution; it will be seen that the characterization of shape from information in the perpendicular and parallel directions can be deceptive.

The Rouse model consists of N beads connected by the set of $N - 1$ vectors $\mathbf{Q}_k$ connecting bead k to bead $k + 1$.[1] Alternately, the chain can be described by $N - 1$ of the N center-of-mass vectors $\mathbf{R}_\nu$, which connect individual beads to the chain center of mass. The nonequilibrium static structure factor for this bead-spring model can be written as

$$P(\theta) = \frac{1}{N^2}\sum_{\nu=1}^{N}\sum_{\mu=1}^{N} < 1 - \frac{[(\mathbf{R}_\nu - \mathbf{R}_\mu)\cdot\mathbf{q}]^2}{2} > \qquad (1)$$

where $< >$ denotes ensemble averaging over all configurations, and $\mathbf{q}$ is the scattering vector with magnitude $q = (4\pi/\lambda)\sin(\theta/2)$ and direction $\mathbf{n}$. Equation 1 is valid for $qR \ll 1$, where R is a characteristic dimension of the molecule in the direction defined by $\mathbf{n}$. After a little manipulation, eq 1 can be rewritten as

$$P(\theta) = 1 - q^2 <\rho^2> \qquad (2)$$

where

$$<\rho^2> = \frac{1}{N}\sum_{\nu=1}^{N} <(\mathbf{R}_\nu\cdot\mathbf{n})^2> \qquad (3)$$

Equation 3 defines the quantity observed in low-angle scattering, the mean-square of the center-of-mass coordinates projected in the direction of the scattering vector. At equilibrium, $<\rho^2>$ reduces to the mean-square radius of gyration divided by 3.

We will now find an explict form of eq 3 for a Rouse chain in homogeneous flow. By use of the notation and definitions of ref 1, the center-of-mass coordinates can be written in terms of connector coordinates $\mathbf{Q}_k$ using the transformation matrix $B_{\nu k}$,

$$\mathbf{R}_\nu = \sum_{k=1}^{N-1} B_{\nu k}\mathbf{Q}_k \qquad (4)$$

Matrix $B_{\nu k}$ obeys the identity

$$\sum_{\nu=1}^{N} B_{\nu k}B_{\nu j} = C_{kj} \qquad (5)$$

where C_{kj} is the Kramers matrix. We will also change from connector coordinates $\mathbf{Q}_k$ to normal coordinates $\mathbf{Q}_m'$ using the matrix Ω_{km}

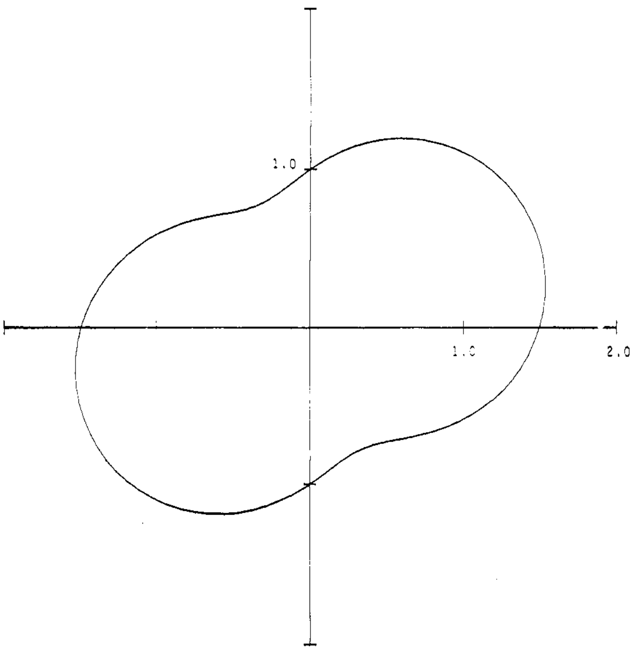

Figure 1. Shape of a 21-bead Rouse chain in shear flow at a dimensionless shear rate of 1.0. A circle of radius 1.0 corresponds to the fully relaxed moelcular shape. The figure is more fully described in the text.

$$\mathbf{Q}_k = \sum_{m=1}^{N-1} \Omega_{km}\mathbf{Q}_m' \qquad (6)$$

The values of Ω_{km} are selected to diagonalize C_{kj}:

$$\sum_{k=1}^{N-1}\sum_{j=1}^{N-1} \Omega_{km}C_{kj}\Omega_{jn} = C_m\delta_{mn} \qquad (7)$$

Using eq 3–7, we obtain an important intermediate result

$$<\rho^2> = \frac{1}{N}\sum_{m=1}^{N-1} C_m\mathbf{nn}{:}<\mathbf{Q}_m'\mathbf{Q}_m'> \qquad (8)$$

The ensemble average in eq 8 can be evaluated from the Kramers expression[1]

$$<\mathbf{Q}_m'\mathbf{Q}_m'> = \frac{1}{nH}(nkT\delta - \tau_m) \qquad (9)$$

where τ_m is the partial stress tensor associated with the mth normal mode, n is the number density of chains, and H is the Hookean spring constant. We obtain our final expression by substitution of eq 9 in eq 8 and writing for the sum over C_m,

$$\sum_{m=1}^{N-1} C_m = \frac{N^2 - 1}{6} \qquad (10)$$

The final result

$$<\rho^2> = \frac{kT}{H}\left(\frac{N^2 - 1}{6N}\right) - \frac{1}{nNH}\sum_{m=1}^{N-1} C_m\mathbf{nn}{:}\tau_m \qquad (11)$$

is valid for any homogeneous, dilute solution flow. The determinations of all parameters on the right-hand side of eq 11 can be found in ref 1.

We have calculated the angular shape of the molecular envelopes defined by eq 11 for steady simple shear and steady uniaxial extension. The results are shown in Figures 1 and 2, where the dimensionless shear and extension rates are 1.0 and 0.45, respectively. The strain rates have been made dimensionless with the longest Rouse relaxation time, and N is 21. In Figure 1, the envelope has been calculated in the plane of shear, with flow being directed

0024-9297/87/2220-2633$01.50/0

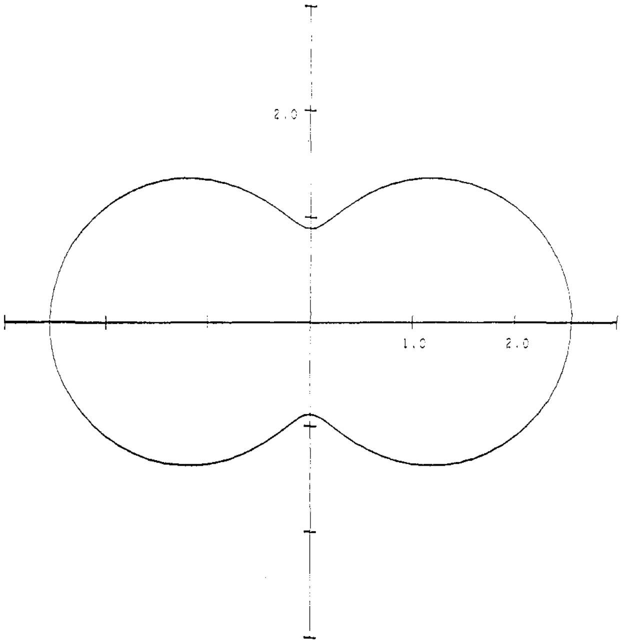

Figure 2. Shape of a 21-bead Rouse chain in uniaxial extension at a dimensionless extension rate of 0.45. See the text for more details.

along the horizontal axis. In Figure 2, the principal axis of extension is aligned along the horizontal axis. In both figures, a circle of radius 1.0 corresponds to the shape of the molecular envelope at equilibrium.

The "dumbbell" shape of the envelopes reveals the difficulty in using the perpendicular low-angle scattering dimension to infer a characteristic transverse length for the stretched molecule. At higher extension rates, where the Rouse model is a less useful depiction of a real macromolecule, the dumbbell shape becomes even sharper. Part of the reason that the scattering approach leads to dumbbell shapes is that averaging is conducted as the *second moment of center-of-mass coordinates integrated* over all beads in a chain. Different averaging procedures, which may not be experimentally accessible, may provide more intuitive, nearly ellipsoidal shapes under the same conditions.[2] The results presented here should not be considered unique to the chosen model, and we expect that dumbbell shapes will be obtained for polymers which are not closely described by the Rouse formulation. Scattering experiments of the type discussed here have been previously reported,[3] and a calculation of scattering in shear flow has been derived previously.[4] Our model, valid only in the small-angle limit, is much simpler and applicable to a broader class of flows. A more accurate description would also consider the effects of hydrodynamic interactions, but the incorporation of nonequilibrium hydrodynamic interactions would appear extremely complex. We have recently become aware of a previous derivation of eq 11 by Roitman and Schrag.[5]

References and Notes

(1) Bird, R. B.; Curtiss, C. F.; Armstrong, R. C.; Hassager, O. *Dynamics of Polymeric Liquids. Vol. 2. Kinetic Theory*, 2nd ed.; Wiley: New York, 1987; Chapter 15.
(2) Hoagland, D. A.; Prud'homme, R. K., submitted for publication in *J. Non-Newtonian Fluid Mech.*
(3) (a) Cottrell, F. R.; Merrill, E. W.; Smith, K. A. *J. Polymer Sci., Part A-2* **1969**, *7*, 1415. (b) Smith, K. A.; Merrill, E. W.; Peebles, L. H.; Banijamali, S. H. In *Polymeres et Lubrification*; C. Wolf, organizer; Colloques Internationaux du CNRS, No. 233; CNRS: Paris, 1975; p 341. (c) Lindner, P.; Oberthur, R. C. *Colloid Polym. Sci.* **1985**, *263*, 443.
(4) Peterlin, A.; Reinhold, C. *J. Chem. Phys.* **1964**, *40*, 1029.
(5) Roitman, D. B.; Schrag, J. L. In *Polymer-Flow Interaction*; Rabin, Y., Ed.; American Institute of Physics Conference Proceedings, No. 137; AIP: New York, 1985; p 77.

Communications to the Editor

New Three-Dimensional Structure for A-Type Starch

Starch granules are the major form for packaging storage carbohydrates in green plants. Most granules exhibit a natural crystallinity due to the local arrangement of linear amylose fragments ($\alpha(1\rightarrow4)$-linked D-glucopyranosyl units), which correspond to the branches of amylopectin, a treelike polymer.[1,2] Two different X-ray patterns can be obtained according to the origin of the granules: A type from cereals and B type from tubers. Previous structural studies on A-type starch have yielded contradictory results: crystallographic data on artificial fibers of amylose resulted in a structure based on antiparallel packing of right-handed double helices,[3] while biochemical data can accommodate only parallel molecules.[4,5]

New crystallographic data were obtained by using two different but interrelated methods: deconvolution of X-ray powder patterns into individual peaks[6] (Figure 1) and electron diffraction on single micron-sized crystals[7] (Figure 2). Samples were prepared by recrystallizing amylose fractions, with a degree of polymerization (DP) of 15, under conditions where the growth of A-type crystals is favored. X-ray diagrams recorded for both samples (polycrystalline powder for X-ray diffraction and micron-sized crystals for electron diffraction) were similar to those displayed by native starch granules but were better resolved. These two new sets of diffraction data, along with that reported by Wu and Sarko[3] yielded the same orthorhombic-like cell (Table I), having a volume of about 2.2 nm^3. According to the measured density of the synthetic crystals, which agrees with the reported density of the fiber, 12 glucose

Table I
Comparison of Cell Dimensions Obtained by Different Diffraction Methods[a]

	orthorhombic cell			monoclinic[b] cell powder X-ray
	fiber X-ray[3]	microcrystal electrons	powder X-ray	
a, nm	1.190	1.116	1.172	2.1245
b, nm	1.770	1.751	1.772	1.172
c, nm	1.052	1.045	1.068	1.068
α, deg	90	90	90	90
β, deg	90	90	90	90
γ, deg	90	90	90	123.48
V, nm^3	2.216	2.042	2.218	2.218
T, °C	20	−170	20	20

[a] The orthorhombic-like cell does not show significant variations from powder and fiber data. However, the electron diffraction data yield a smaller cell; this can be explained by a contraction of the cell due to the very low experimental temperature. [b] The monoclinic cell is deduced by an appropriate transformation of the orthorhombic-like cell derived from the X-ray powder data.

0024-9297/87/2220-2634$01.50/0